

A SELF-CONSISTENT MODEL OF ISOLATED NEUTRON STARS:  
 THE CASE OF THE X-RAY PULSAR RX J0720.4-3125.

J.F. PÉREZ-AZORÍN, J.A. PONS, J.A. MIRALLES  
 Departament de Física Aplicada, Universitat d'Alacant,  
 Ap. Correus 99, 03080 Alacant, Spain

AND

G. MINIUTTI

Institute of Astronomy, University of Cambridge,  
 Madingley Road, Cambridge, CB3 0HA, UK

*Draft version May 25, 2019*

ABSTRACT

We present a unified explanation for the observed properties of the isolated neutron star RX J0720.4-3125 by obtaining, for the first time, a self-consistent model that accounts simultaneously for the observed X-ray spectrum and optical excess, the pulsed fraction, the observed spectral feature around 0.3 keV, and the long-term spectral evolution. By fitting the parameters of our realistic self-consistent models to all archival *XMM-Newton* observations and available optical data, we show that all observed properties are consistent with a *normal* neutron star with a proper radius of about 12 km, a temperature at the magnetic pole of about 100 eV and a magnetic field strength of  $2 - 3 \times 10^{13}$  G, with no need to invoke additional emission and absorption components nor exotic internal composition. The observed variability of the blackbody temperature, strength of the spectral feature, and pulsed fraction are in good agreement with the predictions of our model in which the star is subject to free precession, producing changes in the angle between the magnetic field and the rotation axis of about 10–15 degrees in a few years.

*Subject headings:* Stars: neutron - Stars: magnetic fields - Stars: individual: RX J 0720.4-3125 - Radiation mechanisms: thermal - X-rays: stars

RX J 0720.4-3125 belongs to the family of radio-quiet isolated neutron stars (INS), a puzzling group of compact objects that during the last decade have provoked speculations about their real nature (neutron stars or strange stars) and forced us to reconsider the thermal emission mechanisms. RX J 0720.4-3125 was discovered with ROSAT (Haberl et al. 1997), and its X-ray spectrum was soon found to be well described by a Planckian spectrum with  $kT \approx 82$  eV ( $k$  being the Boltzmann constant). Similarly to the rest of INS, it is a nearby object ( $\approx 300$  pc, Kaplan et al. 2003) and shows low interstellar absorption ( $n_H \approx 1-1.5 \times 10^{20}$  cm $^{-2}$ ). More interestingly, it is a confirmed X-ray pulsar with a period of 8.391 s (Haberl et al. 1997) and it is the only INS with a reliable measure of the period derivative  $\dot{P} = 7 \times 10^{-14}$  ss $^{-1}$  (Kaplan et al. 2005), which implies a magnetic field of about  $B = 2.5 \times 10^{13}$  G. Another important observational property, common to other INS, is that the extrapolation to the optical band of the best blackbody (BB) fit to the X-ray emission results in an apparent optical excess (about a factor of 6). The optical excess flux of INSs, first observed in RX J1865-3754, can be explained with the existence of large temperature anisotropies over the surface (Pons et al. 2002). The evidence of anisotropic temperature distribution is also supported by the observed X-ray pulsations with large pulsation amplitudes ( $\approx 11\%$ ). More recently, the story of INSs has suffered a new twist when observations with XMM-Newton have revealed deviations from a pure BB spectrum in the form of absorption features observed in the 0.1–1.0 keV band. In the particular case of RX J0720.4-3125, a phase dependent absorption line at  $\approx 270$  eV has been

recently reported (Haberl et al. 2004). This feature was associated with a proton cyclotron resonance scattering line requiring a magnetic field of  $\approx 5 \times 10^{13}$  G, consistent within a factor 2 with the dipole breaking estimate. Moreover, this estimate only reflects the large scale magnetic field structure, whereas the presence of smaller scale inner magnetic fields (i.e. strong toroidal components) seems very likely. Strong magnetic fields can affect the emission properties of the neutron star surface in multiple ways. For example, they can induce a phase transition turning the gaseous atmosphere into a solid (Lai 2001), which results in a reduced emissivity compared to a BB. This scenario has been extensively studied by different authors (Brinkmann 1980; Turolla et al. 2004; Pérez-Azorín et al. 2005; van Adelsberg et al. 2005). However, if the magnetic field is high enough to induce the condensation of the atmosphere, it will also lead to very large anisotropies on the surface temperature distribution (Geppert et al. 2004; Pérez-Azorín et al. 2006; Geppert et al. 2006), providing an attractive scenario to naturally explain the observed large optical excess and pulsed fraction of RX J 0720.4-3125.

*The theoretical model.*— In previous papers (Pérez-Azorín et al. 2005, 2006) we have presented the results of detailed calculations of the temperature distribution in the crust and condensed envelopes of neutron stars in the presence of strong magnetic fields, by obtaining axisymmetric, stationary solutions of the heat diffusion equation with anisotropic thermal conductivities. Having explored a variety of magnetic field strengths and configurations, we concluded that variations in the surface temperature of factors 2–10

are easily obtained with  $B \approx 10^{13}\text{--}10^{14}$  G whereas the average luminosity (and therefore the inferred effective temperature) depends only weakly on the strength of the magnetic field. Nevertheless, the luminosity is drastically affected by the geometry, in particular by the existence of a toroidal component of the field. Moreover, the condensed surface models also predict the existence of a spectral edge that for  $B \approx 10^{13}\text{--}10^{14}$  falls in the range 0.2–0.6 keV, and that can be easily misidentified with an absorption line such as that reported in RX J 0720.4–3125 (Haberl et al. 2004). For simplicity, in this work we have considered a force-free magnetic field configuration, but other models with toroidal components give similar results (Pérez-Azorín et al. 2006; Geppert et al. 2006).

The task of fitting observational data in a multi-parameter space is numerically time-consuming (because it requires computing a large number of models to cover a sufficient number of grid points) and theoretically complex (because it is difficult to avoid falling in local minima in a highly dimensional parameter space). For this reason we have not attempted to solve the problem using brute force but rather to discriminate which parameters are more relevant for each observational fact. Our baseline model consists of a neutron star model of  $M = 1.4 M_{\odot}$  and  $R = 12.27$  km, and a force free magnetic field (Pérez-Azorín et al. 2006). The magnetic field strength has been fixed to  $B_{pole} = 2.5 \times 10^{13}$  G, a choice motivated by the inferred value from  $\dot{P}$ .

Having set up a baseline model, we have built tabular XSPEC models<sup>1</sup> as a function of the core temperature for several orientations within the range allowed by the pulsation profiles. We then consider all the available *XMM-Newton* observations of RX J 0720.4–3125 and compare our realistic models to the data and to more phenomenological descriptions of the X-ray spectrum taking also into account the available optical data points.

*Summary of XMM-Newton observations.*— RX J 0720.4–3125 has been observed 7 times by *XMM-Newton* and we focus here on EPIC data (pn and MOS 1). We do not discuss the pn Small Window observations (Rev. 622 and 711) which are much less well calibrated than the Full Frame ones at low energies (see Haberl et al. 2004 who also ignored these data). The pn data of Rev. 078 are also excluded from the analysis due to problems in the SAS 6.5.0 reduction pipeline (see <http://xmm.vilspa.esa.es/> for details). The remaining data provide a homogeneous set and have all been collected with the cameras operated in Full Frame mode with the Thin or Medium filter applied (with the exception of the MOS data of Rev. 175, performed with Large Window and Medium filter). The MOS 2 data are consistent with MOS 1 and do not add relevant information to our analysis. Net exposures range between 22 ks (14 ks) and 27 ks (48 ks) for the pn (MOS 1), a sufficient exposure to provide good quality spectra, given that the source has a 0.1–1 keV flux of  $\simeq 1.1 \times 10^{-11}$  erg cm $^{-2}$  s $^{-1}$ . When present, pile-up has been minimised by extracting product neglecting the innermost brightest 10–15 arc-sec of the source and/or by considering single events only (depending

on the observation science mode and filter). Since the softest energies suffer from calibration uncertainties, we consider the 0.18–1.2 keV band only, after having checked that the inclusion of data down to 0.13 keV does not change our results in any noticeable way (worsening the statistics in a similar way for any spectral model).

*Spectral analysis I: phenomenological fits revisited.*— As already shown by Haberl et al (2004), who analyzed 4 of the 7 EPIC-pn *XMM-Newton* observations, the spectral shape of RX J 0720.4–3125 is not that of a pure absorbed BB. Deviations from a thermal spectrum are seen in the 0.2–0.6 keV band and they are well fitted by models in which a Gaussian absorption line is added to the pure (absorbed) thermal spectrum. The line was interpreted as cyclotron resonance scattering of protons in the NS magnetic field but, in our opinion, it has to be seen as a phenomenological parametrization of the deviations from a BB spectrum. We repeated the analysis by considering all phase-averaged *XMM-Newton* observations and our results are reported in Table 1. Errors are given at the 90% level for one interesting parameter. The Gaussian width cannot be constrained with high confidence and it is fixed to its best-fit average value (75 eV, similar to the 64 eV width imposed by Haberl et al. 2004). The final statistics is good for both cameras and the absorption line is required at more than the 99.99 % confidence level in all observations except Rev. 078, 175, and 622. Our results suggest that the deviations from the thermal spectrum, as inferred from the absorption line equivalent width (EW), are increasing with time, but the only variation that can be claimed with high confidence is that seen in the last observation where the line EW is significantly larger.

We also find a significant variation in the BB temperature with time from  $\sim 85$  eV (Rev. 078–622) to  $\sim 91$  eV in the last two orbits (Rev. 711 and 815), confirming previous works (de Vries et al. 2004; Vink et al. 2004). This may indicate either that the neutron star is getting hotter or, most likely, that the hot spot responsible for the X-ray pulsations of the source, has an increasing effective area (possibly due to changes in the viewing angle produced e.g. by precession), yielding to higher and higher effective temperatures. If so, the pulsed fraction, which reflects the relative intensity of the hot spot emission with respect to the averaged temperature, should also show a correlated increase.

We have then extracted 0.12–1.2 keV light curves for all EPIC-pn observations (including the Small Window ones of Rev. 622 and 711), computed the period of the observed pulsations (always consistent with 8.391 s) and computed the pulsed fraction in each observation. Our results suggest that the pulsed fraction increased from 10–11% to 12–13%. As an example, we measure a pulsed fraction of  $(11.1 \pm 0.4)\%$  in Rev. 533 (Full Frame) and  $(12.5 \pm 0.5)\%$  in Rev. 711 (Small Window). Our results must however be interpreted with caution due to the different science modes used for the pn observations, affecting the pulsed fraction since it does not have uniform spectral shape across the band (Haberl et al. 2004).

*Constraints on the relative orientation.*— Our model mainly depends on the relative orientation between the magnetic axis, the rotation axis, and the observer line of sight. These can be constrained by using the observed pulsed fraction of RX J 0720.4–3125. In Fig. 1 we show

<sup>1</sup> Tabular models are available upon request to the authors

contour plots of the pulsed fraction, for one of our calculations, as a function of the angle between rotation and magnetic axis ( $\mathcal{B}$ ) and rotation and observer direction ( $\mathcal{O}$ ). First, we can classify the light curves in two groups. The models with large  $\mathcal{O} + \mathcal{B}$  are characterized by a non sinusoidal pulsation, or even two visible maxima in the pulse profile; this is because we actually can see both poles in each period if  $\mathcal{O} + \mathcal{B} > 90^\circ$ . We suggest that INSSs which exhibit non-sinusoidal pulse profile do lie in this region. On the other hand, the models with small  $\mathcal{O} + \mathcal{B}$  show always a single peak in the pulse profile which is very close to sinusoidal when either one of the angles is small. This is probably the case of RX J 0720.4-3125, that shows a very regular pulsation profile, indicating that we are seeing only one magnetic pole spinning around the rotation axis. Next, we can reduce the range of angles to those consistent with the observed pulsed fraction. For a nearly spherical neutron star, the rotation axis is essentially aligned with the (vector) total angular momentum of the star, which is conserved. Therefore, the angle  $\mathcal{O}$  is not expected to change with time, but the star can wobble around its symmetry axis (in general different from both, rotation and magnetic axis) with a free precession timescale of a few years for oblateness of the order of  $10^{-7}$  (Jones & Andersson 2001). Therefore, we will focus in the vertical shaded region, fixing  $\mathcal{O}$  and allowing for variations in  $\mathcal{B}$ .

*Spectral analysis II: a self-consistent model.* - We have tried different orientations in the allowed range of variation to found that the data are well reproduced if  $\mathcal{O} = 13^\circ$ , and  $\mathcal{B} = 40 - 60^\circ$ . Notice that this is consistent with a pulsed fraction always in the range 9-13 %. The results of the spectral analysis for *realistic* models, allowing the temperature and the column density to be fit individually for each observation, are summarized in Table 2 and the resulting statistics can be directly compared with the phenomenological fits presented in Table 1. The polar temperature varies approximately from 100 eV to 115 eV, about 15% larger than the BB temperature of Table 1, while the average effective temperature is about 35-41 eV, more than a factor 2 smaller than the BB temperature (see Table 1). This is a result of very large anisotropies over the surface temperature (a factor 10 between pole and equator) induced by the magnetic field. The X-ray spectrum is dominated by the small hot polar area, while the extended cooler equatorial belt is responsible for most of the optical flux. The statistical quality of the fits obtained with the realistic models is comparable to that obtained with BB plus Gaussian models (Table 1) and much better than simple BB models.

Another interesting fact is the variability of the angle  $\mathcal{B}$  between observations.  $\mathcal{B}$  tends to increase from Rev. 078 to Rev 622 and decrease later. By considering the vertical shaded area in Fig. 1, this solution is totally consistent with the pulsed fraction behaviour we suggested with a maximum pulsed fraction around  $\mathcal{B} \sim 55^\circ$ , corresponding to the latest observations.

If the interpretation that all variability is due to free precession of the neutron star is correct, one should be able to find a unique model (temperature, magnetic field configuration, etc.) that explains all observations by only varying the relative orientation and we believe that our model approaches that solution. Our results point in the

direction that most of the variation (if not all) is actually explained by precession of the neutron star. Notice that a precession timescale of a few years has already been reported for some pulsars (Link & Epstein 2001). However, at this stage, we cannot rule out yet that the polar temperature is larger in observation 711 and 815 than before. Notice that the last two observations have also more absorption, so that another possibility is that the neutron star was crossing a small overdense region.

In Fig. 2, we show the unfolded spectra for the best fits to the X-ray spectrum of Rev. 175 (solid line) and 534 (dashes) together with the available optical-UV data (Kaplan et al. 2003). We have not attempted to fit simultaneously the optical and X-ray data, but the good agreement is evident. For comparison, we also show (dotted lines) the best BB plus Gaussian fit for the Rev. 534 data to illustrate its similarity with the realistic model in the X-ray band and to highlight the well known problem of under-predicting the optical flux. The variability of the spectrum with the observation angle is evident ( $\mathcal{B} \simeq 26$  in Rev. 175 and  $\mathcal{B} \simeq 50$  in Rev. 534) in the 0.3-0.4 keV band where the spectral feature is more prominent.

Notice that the best fits to the X-ray observations are in perfect agreement with the optical observations of Jul 2001, but the latter optical observations (Feb 2002) indicate a lower flux than expected. The fact the the optical observations are not consistent with a pure Rayleigh-Jeans tail has been discussed in detail in Kaplan et al. (2003) who found that the best fit consists of two BBs plus a power law. However, they also comment that the spectrum can be consistent with a Rayleigh-Jeans tail if the deviations have a temporal nature. It was thought to be unlikely because the X-ray flux was constant but, as we have discussed above, some temporal variation of the average temperature is not yet ruled out.

*Summary.* - We have shown that realistic models of neutron stars with strong magnetic fields and anisotropic temperature distributions are consistent with both the X-ray and optical spectra, the observed deviation from a pure thermal spectrum in the X-ray band, and the long term variability. Although we cannot rule out the presence of a proton cyclotron line, we do not need to invoke it to explain the observed spectral and temporal properties. For a given magnetic field configuration, we are able to obtain a self-consistently calculated thermal spectrum that reproduces reasonably well all available observations. Our analysis indicates that most of the long-term spectral variation of the source can be explained in terms of neutron star precession. If our interpretation is correct, we predict that the pulsed fraction, effective temperature, and absorption line equivalent width as obtained with phenomenological models, will start to decrease (with respect to the values obtained in Rev. 711 and 815) in subsequent observations of the source.

Since we have only explored a few parameters of our model ( $B, T, \mathcal{B}$ ), an extended grid of spectral models is very likely to improve the statistical quality of the fits presented here. We are working to attack other INSSs that we expect to be well described by our models. Our goal is to derive a simple and reasonable solution towards a unified picture in which INSSs are just old, cold magnetars whose magnetic fields are a few times smaller than usual,

TABLE 1  
THE PN AND MOS 1 DATA FOR ALL OBSERVATIONS ARE FITTED IN THE  
0.18–1.2 keV BAND WITH AN ABSORBED BB MODEL INCLUDING A  
GAUSSIAN ABSORPTION LINE.

Rev.–Det.	$n_H$ $10^{20}$ cm $^{-2}$	kT (eV)	$E_{\text{line}}$ (eV)	$-EW_{\text{line}}$ (eV)	$\chi^2/\text{dof}$
078–pn	—	—	—	—	—
078–mos1	$0.72^{+0.35}_{-0.33}$	$84.4^{+1.1}_{-1.8}$	$340^{+140}_{-165}$	< 20	58/53
175–pn	$0.82^{+0.28}_{-0.42}$	$83.7^{+0.7}_{-1.2}$	$249^{+102}_{-105}$	< 40	141/152
175–mos1	$0.92^{+0.30}_{-0.47}$	$85.0^{+1.4}_{-1.0}$	$306^{+120}_{-100}$	< 40	70/55
533–pn	$1.20^{+0.11}_{-0.27}$	$85.0^{+1.1}_{-1.0}$	$297^{+22}_{-19}$	$32^{+11}_{-10}$	178/160
533–mos1	$1.20^{+0.25}_{-0.57}$	$87.0^{+1.9}_{-1.8}$	$301^{+53}_{-40}$	$35^{+25}_{-24}$	58/50
534–pn	$1.05^{+0.19}_{-0.42}$	$85.7^{+1.1}_{-1.1}$	$308^{+18}_{-22}$	$35^{+8}_{-6}$	159/162
534–mos1	$0.82^{+0.31}_{-0.36}$	$86.5^{+1.3}_{-2.5}$	$320^{+50}_{-35}$	$25^{+18}_{-18}$	69/51
622–pn	—	—	—	—	—
622–mos1	$1.40^{+0.32}_{-0.82}$	$86.5^{+2.2}_{-1.9}$	$350^{+130}_{-150}$	< 50	46/48
711–pn	—	—	—	—	—
711–mos1	$1.80^{+1.05}_{-1.10}$	$90.3^{+2.2}_{-2.8}$	$370^{+40}_{-55}$	$45^{+23}_{-21}$	47/47
815–pn	$1.32^{+0.35}_{-0.19}$	$91.4^{+1.1}_{-1.2}$	$308^{+11}_{-9}$	$70^{+7}_{-9}$	160/163
815–mos1	$1.72^{+0.63}_{-1.05}$	$91.0^{+2.8}_{-2.9}$	$370^{+20}_{-20}$	$50^{+20}_{-15}$	50/52
tot–pn	—	—	—	—	$\chi^2_r = 1.00$
tot–mos1	—	—	—	—	$\chi^2_r = 1.26$

maybe because they have decayed during their lifetime.

#### REFERENCES

Brinkmann, W. 1980, A&A 82, 352  
 de Vries, C.P., et al., 2004, A&A, 415, L34  
 Geppert, U., Küker, M., & Page, D. 2004, A&A, 426, 267  
 Geppert, U., Küker, M., & Page, D. 2006, A&A, [arXiv:astro-ph/0512530]  
 Haberl, F., Motch, C., Buckley, D. A. H., Zickgraf, F. J., & Pietsch, W. 1997, A&A, 326, 662  
 Haberl, F., Zavlin, V.E., Trümpre, J., Burwitz, V., 2004, A&A, 419, 1077  
 Jones, D.I. & Andersson, N., 2001, MNRAS, 324, 811  
 Link, B. & Epstein, R.I., 2001, ApJ, 556, 392  
 Kaplan, D.L. et al., 2003, ApJ, 590, 1008  
 Kaplan, D.L. & van Kerkwijk, M.H., 2005, ApJ, 628, L45  
 Lai, D. 2001, Rev. of Mod. Phys., 73, 629  
 Pérez-Azorín, J.F., Miralles J.A., & Pons J.A. 2005, A&A, 433, 275  
 Pérez-Azorín, J.F., Miralles J.A., & Pons J.A. 2006, A&A, in press [arXiv:astro-ph/0510684]  
 Pons, J.A., Walter, F.M., Lattimer, J.M. et al. 2002, ApJ, 564, 981  
 Turolla, R., Zane, S., & Drake, J.J. 2004, ApJ, 603, 265  
 van Adelsberg, M., Lai, D., & Potekhin, A. 2005, ApJ, 628, 902  
 Vink, J., de Vries, C.P., Méndez, M., & Verbunt, F. 2004, ApJ, 609, L75

TABLE 2  
THE PN AND MOS 1 DATA FOR ALL OBSERVATIONS ARE FITTED IN THE 0.18–1.2 keV BAND WITH A REALISTIC MODEL WITH  $\mathcal{O} = 13^\circ$  AND  $B = 2.5 \times 10^{13}$  G.

Rev.–Det.	$n_H$ $10^{20}$ cm $^{-2}$	$B$	$kT_{pole}$ (eV)	$R_\infty/D_{300}$ (km/300 pc)	$\chi^2/dof$
078–pn	–	–	–	–	–
078–mos1	$0.81^{+0.12}_{-0.07}$	$43^{+4}_{-5}$	100	$15^{+5}_{-4}$	70/55
175–pn	$0.93^{+0.08}_{-0.08}$	$26^{+4}_{-6}$	103	$13^{+3}_{-3}$	149/154
175–mos1	$0.8^{+0.2}_{-0.2}$	$40^{+4}_{-5}$	103	$14^{+4}_{-4}$	59/57
533–pn	$1.86^{+0.07}_{-0.09}$	$46^{+2}_{-3}$	103	$16^{+3}_{-4}$	180/162
533–mos1	$1.4^{+0.3}_{-0.3}$	$48^{+5}_{-6}$	106	$14^{+4}_{-4}$	53/52
534–pn	$1.87^{+0.07}_{-0.07}$	$50^{+2}_{-2}$	103	$16^{+4}_{-3}$	165/164
534–mos1	$0.8^{+0.2}_{-0.2}$	$51^{+4}_{-5}$	103	$15^{+5}_{-5}$	66/53
622–pn	–	–	–	–	–
622–mos1	$1.7^{+0.3}_{-0.2}$	$59^{+4}_{-5}$	101	$18^{+5}_{-7}$	47/50
711–pn	–	–	–	–	–
711–mos1	$2.1^{+0.4}_{-0.4}$	$55^{+6}_{-5}$	113	$13^{+5}_{-4}$	59/49
815–pn	$2.51^{+0.1}_{-0.09}$	$50^{+3}_{-1}$	113	$13^{+3}_{-2}$	270/165
815–mos1	$2.2^{+0.3}_{-0.3}$	$55^{+5}_{-3}$	113	$12^{+4}_{-3}$	73/54
tot–pn	–	–	–	–	$\chi^2_r = 1.18$
tot–mos1	–	–	–	–	$\chi^2_r = 1.15$

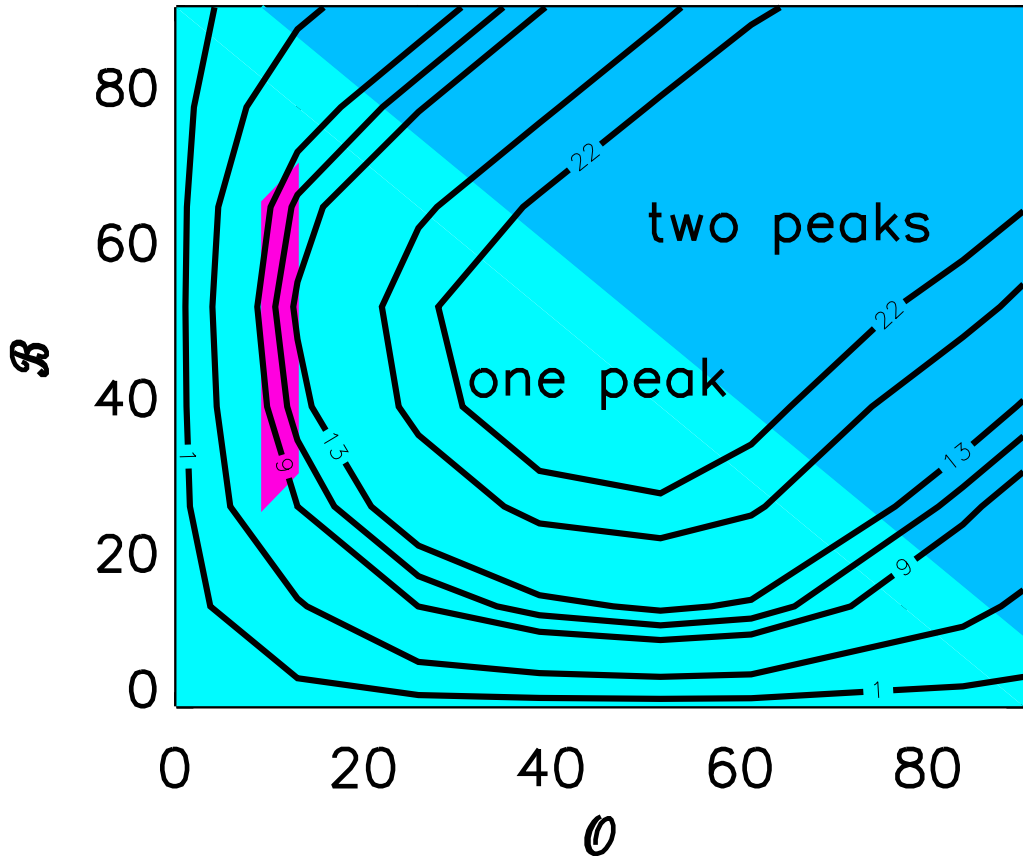


FIG. 1.— Contour plots of the pulsed fraction for a realistic surface temperature distribution.  $B$  is the angle between rotation and magnetic axis, and  $\mathcal{O}$  the angle between the rotation axis and the observer direction. The flux has been obtained by integration over the whole surface taking into account General Relativistic light bending effects.

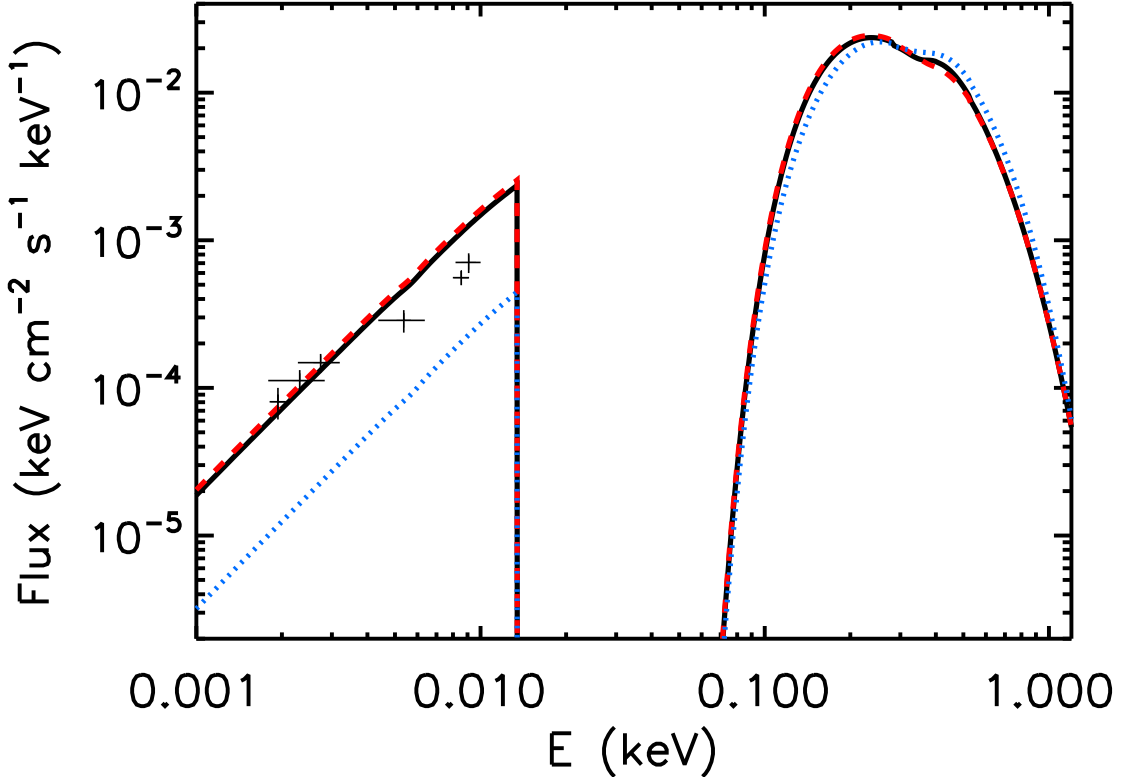


FIG. 2.— Spectral energy distribution of the best fits for revolutions 175 (solid line) and 534 (dashes), compared with the best BB+Gaussian fit (dots) of orbit 534. Optical and UV data (Kaplan et al. 2003) are also shown for comparison.